

Exploring the partonic collectivity in small systems at the LHC

Yuanyuan Wang,¹ Wenbin Zhao,^{2,3,*} and Huichao Song^{1,4,†}

¹*School of Physics, Peking University, Beijing 100871, China*

²*Nuclear Science Division, Lawrence Berkeley National Laboratory, Berkeley, California 94720, USA*

³*Physics Department, University of California, Berkeley, California 94720, USA*

⁴*Center for High Energy Physics, Peking University, Beijing 100871, China*

(Dated: January 3, 2024)

Using the **Hydro-Coal-Frag** model that combines hydrodynamics at low p_T , quark coalescence at intermediate p_T , and the **LBT** transport model at high p_T , we study the spectra and elliptic flow of identified hadrons in high multiplicity p-Pb and p-p collisions at the Large Hadron Collider (LHC). In p-Pb collisions, the **Hydro-Coal-Frag** model gives a good description of the differential elliptic flow over the p_T range from 0 to 6 GeV and the approximate number of constituent quark (NCQ) scaling at intermediate p_T . Although **Hydro-Coal-Frag** model can also roughly describe the elliptic flow in high multiplicity p-p collisions with the quark coalescence process, the larger contribution from the string fragmentations leads to a notable violation of the NCQ scaling of v_2 at intermediate p_T as observed in the experiment. Comparison runs of the **Hydro-Frag** model without the coalescence process demonstrate that regardless the parameter adjustments, the **Hydro-Frag** model cannot simultaneously describe the p_T spectra and the elliptic flow of identified hadrons in either p-Pb collisions or p-p collisions. The calculations in this paper thus provide support for the existence of partonic degrees of freedom and the possible formation of the QGP in the small systems created at the LHC.

PACS numbers: 25.75.Ld, 25.75.Gz

I. INTRODUCTION

The main goals of the heavy ion program at the Relativistic Heavy Ion Collider (RHIC), and the Large Hadron Collider (LHC) are to create and study the quark-gluon plasma (QGP), a state of hot and dense nuclear matter in which quarks and gluons are no longer bound into hadrons. Since the running of 200 A GeV Au-Au collisions at RHIC, many signals of the QGP have been observed, such as the collective flow, valence quark scaling and jet quenching [1–5]. It was found that the QGP droplet created in relativistic heavy ion collisions is the most perfect liquid in nature, with collective features well described by the relativistic hydrodynamics [6–10].

For small systems, the multi-particle correlations in high multiplicity p-Pb, and p-p collisions at the LHC have exhibited surprising collective behaviors, including the long-range double-range structures in two-particle correlations [11–18], four-particle cumulant $c_2\{4\}$ turning to negative values in high multiplicity events [13–15, 19, 20], and mass splitting of elliptical flow among different hadron species [19, 21, 22]. In the past ten years, various models have been applied to explain the emergence of collectivity in the small systems. Hydrodynamic models based on final state interactions [23–39] and the Color Glass Condensate (CGC) model based on initial state correlations [40–51] can both qualitatively describe the collective flow in the low transverse momentum region. In the high transverse momentum region,

jet quenching, the hard probe signals for the QGP formation, has not been observed due to the limited size and lifetime of the small systems. The experimentally observed hadron suppression factor R_{pA} of the small system is consistent with the calculations from the cold nuclear effect [52, 53].

In the intermediate transverse momentum regime, the ALICE and CMS collaborations have observed an approximate number of constituent quark (NCQ) scaling of v_2 for identified hadrons in high multiplicity p-Pb collisions at the LHC [54, 55]. Meanwhile, the **Hydro-Coal-Frag** model that includes various hadronization mechanisms from hydrodynamics, quark coalescence, and the **LBT** string fragmentations in different transverse momentum regimes has been developed. It has well described the transverse momentum spectrum and differential elliptic flow for identified hadron from 0 to 6 GeV in p-Pb and Pb-Pb collisions [56–58] and explained the NCQ scaling of v_2 in p-Pb collisions with the quark coalescence process.

Recently, the CMS, ATLAS and ALICE collaborations have measured the p_T -spectra and $v_2(p_T)$ of all charged and identified hadrons in high multiplicity p-p collisions at $\sqrt{s_{NN}} = 13$ TeV [19, 59, 60]. In this paper, we will perform the first systematic study of the elliptic flow over the transverse momentum region from 0 to 6 GeV in both high multiplicity p-p and p-Pb collisions. We will show that, with the quark coalescence process, the **Hydro-Coal-Frag** model describes the elliptic flow of various hadron species in both p-p and p-Pb collisions, which also gives an approximate NCQ scaling of v_2 at intermediate p_T in p-Pb collisions. While the larger contribution from the string fragmentations leads to a notable violation of the NCQ scaling of v_2 in p-p

* Wenbin Zhao: WenbinZhao@lbl.gov

† Huichao Song: huichaosong@pku.edu.cn

collisions as observed in the experiment. Compared to our early short paper [56], we will also explain more details about the Hydro-Coal-Frag model for the sake of documentation and easiness of reading.

II. THE MODEL AND SET-UPS

Relativistic heavy ion collision is a dynamical evolution process, which is consistent with the initial state, pre-equilibrium dynamics, thermalization, the QGP expansion, hadronization, hadronic evolution, and the chemical and kinematic freeze-out. In this work, we implement the Hydro-Coal-Frag model, which produces low p_T hadrons from hydrodynamics, high p_T hadrons from fragmentations and intermediate p_T hadrons from the coalescence process [56]. Here, the initial entropy distributions are generated by a parameterized initial condition model TRENTo (Reduced Thickness Event-by-Event Nuclear Topology) [61], and the evolution of the QGP is described by a (2+1)-dimensional viscous hydrodynamics (VISH2+1) [62–66], which produces thermalized hadrons and partons at low p_T from the freeze-out surface near T_c . The initial hard partons are produced by PYTHIA8 [67], and the interaction between the initial hard partons and the bulk thermal medium is modeled by the linear Boltzmann transport model (LBT) [68–71], which includes both pQCD elastic scattering and medium-induced gluon radiation within the high-twist approach. Hadron production at intermediate p_T is described by the parton coalescence model, which includes thermal-thermal, thermal-hard, and hard-hard partons recombinations with the remaining hard partons hadronized by string fragmentation [56, 57]. Finally, these produced hadrons at different p_T regimes are fed to the Ultra-relativistic Quantum Molecular Dynamics (UrQMD) for subsequent hadronic evolution with scatterings and resonance decays [72].

More specifically, for soft hadron production at low p_T , we implement a 2+1D viscous fluid model, VISH2+1, with longitudinal boost-invariance to simulate the collective expansion of the QGP, which numerically solves the transport equations of the energy-momentum tensor $T^{\mu\nu}$ and the evolution equations of the shear viscous tensor $\pi^{\mu\nu}$ and the bulk viscous pressure Π in the second-order [63–65, 73]. To close the systems, we input the equation of state s95-PCE [74, 75], and start the hydrodynamic simulations at $\tau = 0.8$ fm/c with the TRENTo model, which parameterizes the initial entropy density by the thickness functions $T_{A/B}$: $s = s_0[(T_A^p + T_B^p)/2]^{1/p}$. Here, p is an adjustable parameter that allows TRENTo to effectively transit between different initial conditions, such as KNL, EKRT, WN, etc. [61, 76]. In this paper, we implement the version of TRENTo with sub-nucleonic structures [76, 77]. So that the thickness function is written as $T(x, y) \equiv \int dz \frac{1}{n_c} \sum_{i=1}^{n_c} \gamma_i \rho_c(\mathbf{x} - \mathbf{x}_i \pm \mathbf{b}/2)$, where n_c is the number of constituents in a nucleon, ρ_c is the density of the constituent with a Gaussian form:

$\rho_c = (2\pi w_c^2)^{-3/2} \exp[-\mathbf{x}^2/(2w_c^2)]$, γ_i is a random weighting factor with a unit mean and variance $1/\sigma_{\text{flut}}$, \mathbf{x}_i is the position of the constituent and \mathbf{b} is the impact parameter. As the QGP fireball expands and cools down, the hydrodynamic system hadronizes near T_c , which is realized by the iSS event generator [78] that produces thermal hadrons on the freeze-out surface according to the Cooper-Frye formula [78]. For the following quark coalescence process at intermediate p_T , we also sample the thermal partons at low p_T from the hydrodynamic freeze-out surface near T_c .

Following the early model calculations [56, 57, 79–83], we set the mass of the thermal quark to $m_{u,d} = 0.25$ GeV, $m_s = 0.43$ GeV, and convert the thermal gluons into to quark and anti-quark pairs via $gg \rightarrow q\bar{q}$. For p-p collisions at $\sqrt{s_{\text{NN}}} = 13$ TeV, the TRENTo parameters are set to: the normalization factor $s_0 = 20$, the reduced thickness $p = 0$, the fluctuation $\sigma_{\text{flut}} = 0.19$, the nucleon width $r_{\text{cp}} = 0.92$ fm, the constituent width $w_c = 0.6$ fm, and the constituent number $n_c = 6$ [76]. We also tune the specific shear and bulk viscosity and the hydrodynamic switching temperature to: $\eta/s = 0.03$, $\zeta/s = 0.4$ and $T_{\text{switch}} = 150$ MeV in order to fit the soft p_T -spectra and elliptic flow blow 2 GeV. For p-Pb collisions at $\sqrt{s_{\text{NN}}} = 5.02$ TeV, the TRENTo parameters are the same as the p-p collisions except that the constituent width is changed to $w_c = 0.4$ fm, and the switching temperature is set to: $T_{\text{switch}} = 160$ MeV. The specific shear and bulk viscosity are tuned as: $\eta/s = 0.12$ and $\zeta/s = 0.6$ to fit the new ALICE flow data in p-Pb collisions obtained by the “template fit” method [84]. Note that, due to the different non-flow subtraction assumptions, the “template fit” results generally have larger flow magnitudes than those obtained from the “peripheral subtraction” method used by the CMS collaboration [55].

For hard parton production, we implement PYTHIA8 [67] to produce the initial hard partons, and then feed them into the LBT model to simulate their propagation in the bulk medium. The LBT model solves the linear Boltzmann equations for quarks, antiquarks, and gluons with elastic scatterings, inelastic scatterings and medium-induced gluon radiation within an expanding QGP described by hydrodynamics [68–71, 85, 86]. For p-Pb collisions, the nuclear shadowing effects on the momentum space distribution of the initial hard partons inside the lead have been parameterized by EPPS16 in PYTHIA8 [53]. The only tunable parameter in LBT is the strong coupling constant α_s , which is set to $\alpha_s = 0.15$ that has been tuned to fit the R_{AA} and the anisotropic flow of light and heavy flavors at high p_T for Au-Au collisions and Pb-Pb collisions at RHIC and the LHC [87, 88]. The virtualities of hard gluons are generally set to be zero in LBT. Following [89], we assume that the hard gluon has a virtual mass uniformly distributed between $2m_s$ and m_{max} , where m_s is the mass of the strange quark, and m_{max} is a tunable parameter that determines the ratio of light to strange quarks for the following quark coalescence calculations.

According to Ref. [56], we set $m_{\max} = 1.5$ GeV to fit the relative spectra between kaon and pion at intermediate p_T in our model calculations. With virtual masses, the hard gluons decay isotropically into $q\bar{q}$ pairs, with $u\bar{u}$ and $d\bar{d}$ pairs had equal decay weight, and the ratio of light to strange quarks given by the associated phase space. These final partons are then either fed into the following coalescence model calculations or form hard hadrons through string fragmentations.

For hadron production at intermediate p_T , we implement the quark coalescence model, which combines thermal-thermal, thermal-hard, and hard-hard partons obtained from the hydrodynamic freeze-out and the LBT parton shower evolution. Using the thermal and hard parton distributions, obtained from the VISH2+1 and LBT models, the momentum distributions of mesons and baryons from coalescence are generated from an overlap of the Wigner functions [89]:

$$\begin{aligned} \frac{dN_M}{d^3P_M} &= g_M \int d^3\mathbf{x}_1 d^3\mathbf{p}_1 d^3\mathbf{x}_2 d^3\mathbf{p}_2 f_q(\mathbf{x}_1, \mathbf{p}_1) f_{\bar{q}}(\mathbf{x}_2, \mathbf{p}_2) \\ &\quad \times W_M(\mathbf{y}, \mathbf{k}) \delta^{(3)}(\mathbf{P}_M - \mathbf{p}_1 - \mathbf{p}_2), \\ \frac{dN_B}{d^3P_B} &= g_B \int d^3\mathbf{x}_1 d^3\mathbf{p}_1 d^3\mathbf{x}_2 d^3\mathbf{p}_2 d^3\mathbf{x}_3 d^3\mathbf{p}_3 \\ &\quad \times f_{q_1}(\mathbf{x}_1, \mathbf{p}_1) f_{q_2}(\mathbf{x}_2, \mathbf{p}_2) f_{q_3}(\mathbf{x}_3, \mathbf{p}_3) \\ &\quad \times W_B(\mathbf{y}_1, \mathbf{k}_1; \mathbf{y}_2, \mathbf{k}_2) \delta^{(3)}(\mathbf{P}_B - \mathbf{p}_1 - \mathbf{p}_2 - \mathbf{p}_3). \end{aligned}$$

where f_q and $f_{\bar{q}}$ are the phase-space distributions of quarks and anti-quarks, W_M and W_B are the Wigner functions of the meson and the baryon, \mathbf{y} and \mathbf{k} are the relative coordinates and relative momenta between the valence quarks in the local rest frame of the meson. According to Ref. [89], the Wigner function of meson in the n -th excited state is $W_{M,n}(\mathbf{y}, \mathbf{k}) = v^n e^{-v} / n!$, where $v = (\mathbf{y}^2 / \sigma_M^2 + \mathbf{k}^2 \sigma_M^2) / 2$. The Wigner function of a baryon in the n_1 -th and n_2 -th excited states is given by $W_{B,n_1,n_2}(\mathbf{y}_1, \mathbf{k}_1; \mathbf{y}_2, \mathbf{k}_2) = v_1^{n_1} e^{-v_1} v_2^{n_2} e^{-v_2} / (n_1! n_2!)$, where $v_i = (\mathbf{y}_i^2 / \sigma_{B_i}^2 + \mathbf{k}_i^2 \sigma_{B_i}^2) / 2$ with \mathbf{y}_i and \mathbf{k}_i being the relative coordinates and momenta among the three constituent quarks in the local rest frame of the baryon. Following Refs. [56, 58], we take the excited meson states up to $n = 10$ and the excited baryon states up to $n_1 + n_2 = 10$ [89]. The width parameters σ_M , σ_{B_1} and σ_{B_2} are determined by the radii of formed hadrons from the Particle Data Group [90]. After the thermal-thermal, thermal-hard, and hard-hard partons have recombined, the remaining hard partons that do not have coalescence partners are connected with strings, which then perform the string fragmentation of the hadron standalone mode in PYTHIA8 to form hard hadrons [67]. For more details, please refer to [56, 89].

In short, the Hydro-Coal-Frag model combines hydrodynamics to produce low p_T hadrons, quark coalescence model to produce intermediate p_T hadrons, and LBT string fragmentations to produce high p_T hadrons. After the system has completed all the hadronization processes, the subsequent hadronic evolution is simulated by

UrQMD [72], which propagates hadrons with elastic and inelastic scatterings and resonance decays until the system becomes very dilute with a kinetic freeze-out. To avoid double counting within Hydro-Coal-Frag, we set a p_T cut-off between hadrons produced by hydrodynamics and those produced by quark coalescence. We only recombine these thermal partons with transverse momentum $p_T > p_{T_1}$ and produce thermal mesons and thermal baryons below $2p_{T_1}$ and $3p_{T_1}$ with hydrodynamics. Meanwhile, for the LBT evolution and fragmentations, we count only these final hard hadrons with transverse momentum $p_T > p_{T_2}$ to avoid overcounting with these low p_T hadrons produced from hydrodynamics. The two parameters p_{T_1} and p_{T_2} and the above parameter m_{\max} for gluon virtuality are determined by fitting the transverse momentum spectrum of π , K, and P and the P/ π ratio at the transition range $p_T \sim 2 - 4$ GeV in the high multiplicity events. Here we find $p_{T_1} = 1.4$ GeV and $p_{T_2} = 2.0$ GeV for p-p collisions and $p_{T_1} = 1.6$ GeV and $p_{T_2} = 2.6$ GeV for p-Pb collisions, together with $m_{\max} = 1.5$ GeV, can well describe these measured p_T spectra in the high multiplicity. With the fixed parameters described above, we further predict the differential elliptic flow of π , K, and P and the associated NCQ scaling for $105 < N_{ch} < 150$ for p-p collisions at $\sqrt{s_{NN}} = 13$ TeV and for 0-20% centrality p-Pb collisions at $\sqrt{s_{NN}} = 5.02$ TeV. For comparison, we also perform the calculations from the Hydro-Frag model, which includes only hydrodynamics and string fragmentations but without the quark coalescence process.

III. RESULTS AND DISCUSSIONS

The left panels (a) and (c) of Fig. 1 show the transverse momentum spectra of π , K and P in 0-20% p-Pb collisions at $\sqrt{s_{NN}} = 5.02$ TeV and in 0-0.92% p-p collisions at $\sqrt{s_{NN}} = 13$ TeV, calculated from the Hydro-Coal-Frag model with the coalescence process. With properly tuned parameters, the model gives good descriptions of the transverse momentum spectra of π , K and P over the p_T range from 0 to 6 GeV. It also nicely describes the P/ π ratio as a function of p_T , showing an increasing then a decreasing trend, as observed by the ALICE collaboration. The two right panels (b) and (d) show the calculated p_T spectra from the Hydro-Coal-Frag model with the individual contributions from hydrodynamics, quark coalescence and string fragmentation. It demonstrates that hadrons produced at low or high transverse momentum are dominantly contributed by hydrodynamics or the string fragmentation respectively. At intermediate p_T regime, both quark coalescence and string fragmentation contribute to the hadron productions. It is noteworthy that the relative yield from quark coalescence is more pronounced in p-Pb collisions than in p-p collisions. Specifically, in p-Pb collisions, the yield of coalescence hadrons is close to that of fragmentation hadrons at intermediate p_T , while in p-p

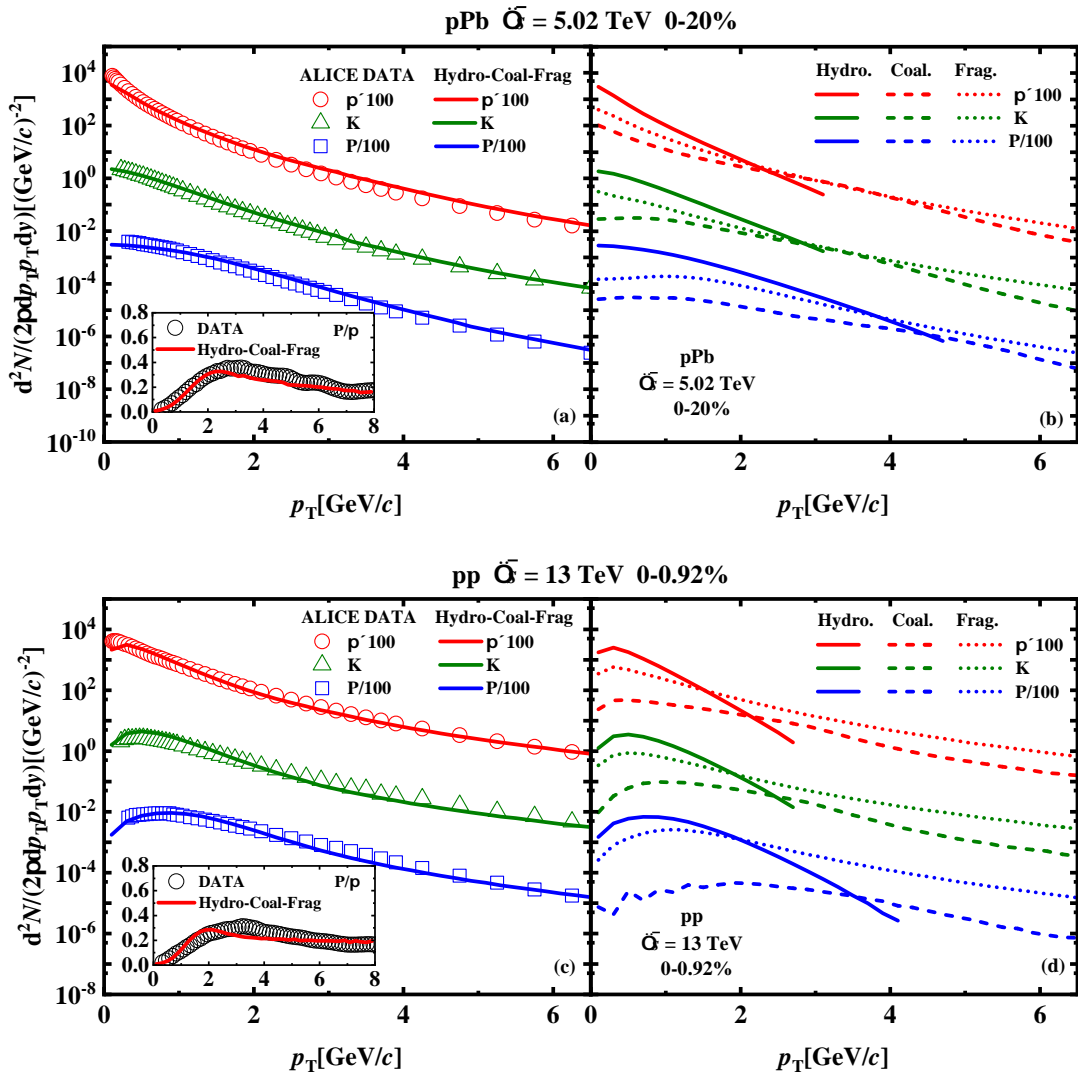


FIG. 1. (Color online) Left panel: transverse momentum spectra of π , K and P calculated from the Hydro-Coal-Frag model, with the inset panels showing the proton-to-pion ratio. Right panel: the contributions from hydrodynamics (solid lines), quark coalescence (dashed lines), and string fragmentation (dotted lines) processes. Upper and bottom panels are for 0-20% p-Pb collisions at $\sqrt{s_{NN}} = 5.02$ TeV and for 0-0.92% p-p collisions at $\sqrt{s_{NN}} = 13$ TeV, respectively. The data are from the ALICE papers [59, 91].

collisions, coalescence hadrons is below 50% of the fragmentation hadrons. This difference is due to the larger QGP droplet in p-Pb collisions, which generates more thermal partons and leads to a larger yield of coalescence hadrons than that in p-p collisions. With these different hadron production procedures that smoothly transit among different transverse momentum regimes, the Hydro-Coal-Frag model can well describe the p_T spectra of π , K and P from 0-6 GeV in both p-Pb and p-p collisions.

Figure. 2 shows the differential elliptic flow $v_2(p_T)$ of π , K, P and Λ in 0-20% p-Pb collisions at $\sqrt{s_{NN}} = 5.02$ TeV and in $105 < N_{ch} < 150$ p-p collisions at $\sqrt{s_{NN}} = 13$ TeV, calculated from the Hydro-Coal-Frag model and

the Hydro-Frag model, respectively. As a full hybrid model that includes hydrodynamics, quark coalescence and string fragmentation at different transverse momentum regimes, Hydro-Coal-Frag provides a reasonable description of the elliptic flow of identified hadrons over the p_T range from 0 to 6 GeV for both p-Pb and p-p collisions. At low p_T , hadron productions from Hydro-Coal-Frag are dominated by hydrodynamics, which leads to a clear mass ordering of $v_2(p_T)$ among different hadron species. At intermediate p_T , the elliptic flow calculated with the quark coalescence process shows a grouping behavior for baryons and mesons, where $v_2(p_T)$ of π and K roughly overlap and $v_2(p_T)$ of P and Λ roughly overlap above 2.5 GeV. The experimental data

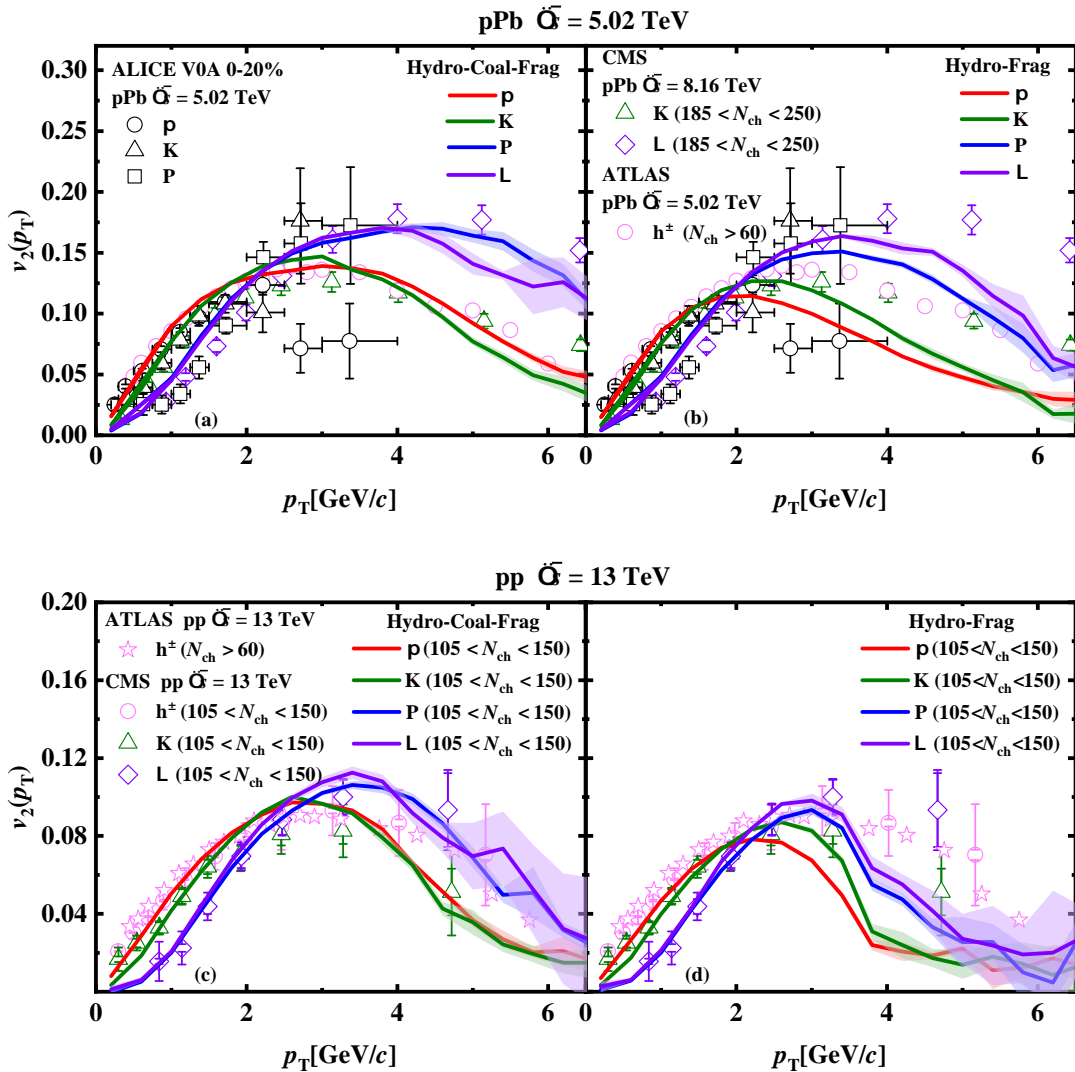


FIG. 2. (Color online) The differential elliptic flow of π , K, P and Λ in 0-20% p-Pb collisions at $\sqrt{s_{NN}} = 5.02$ TeV (upper panel) and in $105 < N_{ch} < 150$ p-p collisions at $\sqrt{s_{NN}} = 13$ TeV (bottom panel), calculated from the **Hydro-Coal-Frag** model and the **Hydro-Frag** model, respectively. Data are from the CMS, ATLAS, and ALICE papers [19, 21, 55, 60].

from the CMS and ALICE collaboration also show a similar grouping tendency for baryons and mesons, but need further confirmation with high statistical run data in the near future. In contrast, the **Hydro-Frag** model largely underestimates $v_2(p_T)$ of hadrons for $3 < p_T < 6$ GeV. In this calculation without the quark coalescence contribution, the splitting of elliptic flow among different hadron species arises primarily from their different masses. In particular, regardless of the adjustments of parameters, the **Hydro-Frag** model cannot simultaneously describe the transverse momentum spectrum and the differential elliptic flow of identified hadrons in either p-Pb or p-p collisions. Note that the quark coalescence procedure in **Hydro-Coal-Frag** transfers the partonic collectivity at low p_T to hadronic collectivity at the intermediate p_T . Our calculation highlights the importance of the partonic

collectivity for describing the differential elliptic flow of light hadrons at the intermediate p_T regions in small systems. It is noteworthy that the enhanced hadron v_2 at $p_T \approx 5 - 6$ GeV in the **Hydro-Coal-Frag** model results from the order of magnitude larger v_2 from coalescence compared to those from fragmentation. Although more hadrons are produced by fragmentation than by coalescence at these momenta, the larger v_2 from coalescence hadrons contributes significantly to the observed enhancement of v_2 at high p_T in p-Pb and p-p collisions.

In Fig. 3, we further study the number of the constituent quark scaling of the elliptic flow in the small systems. The top and bottom panels show the number of constituent quark scaled elliptic flow $v_2(p_T)/n$ ($n = 2$ for mesons and $n = 3$ for baryons) in 0 - 20% p-Pb collisions at $\sqrt{s_{NN}} = 5.02$ TeV and in $105 < N_{ch} < 150$ p-p col-

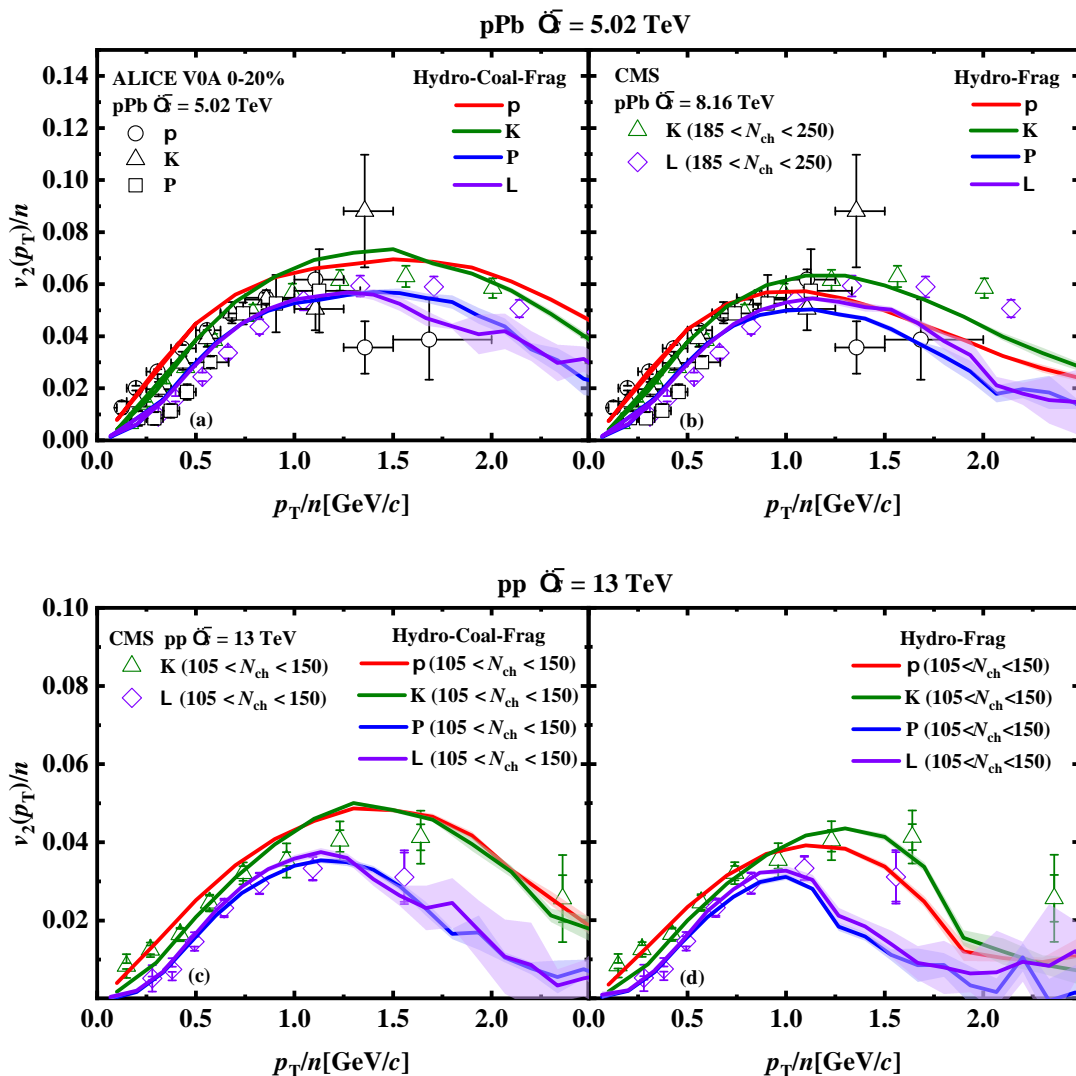


FIG. 3. (Color online) Similar to Fig. 2, but for the number of constituent quark (NCQ) scaled $v_2(p_T)$ of π , K, P and Λ .

lisions at $\sqrt{s_{NN}} = 13$ TeV, respectively. With the quark coalescence included, the **Hydro-Coal-Frag** model gives an approximate NCQ scaling behavior in the transverse momentum region $1.2 < p_T/n < 2$ for p-Pb collisions. This result is in agreement with the ALICE measurements. In our calculations, we also observe a slight break of the NCQ scaling, which is due to the contribution from the string fragmentations and resonance decays. In the case of p-p collisions, the break of the NCQ scaling behavior is more noticeable for both the **Hydro-Coal-Frag** results and the experimental measurements. As shown in Figure 1, the quark coalescence contributions at intermediate p_T are smaller in p-p collisions than in p-Pb collisions, leading to a larger violation of the NCQ scaling in p-p collisions. For comparison, we also perform the **Hydro-Frag** model calculations without the quark coalescence process. As shown in the two right panels of Fig. 3, not only is the NCQ scaling behavior at the

intermediate transverse momentum region violated, but also the magnitude of $v_2(p_T)/n$ is significantly underestimated for both p-Pb and p-p collisions. Compared to the experimental data, the **Hydro-Frag** model gives a reduced $v_2(p_T)/n$ for each hadron species by more than 20-50% in p-Pb and p-p collisions. This indicates that the quark coalescence process is important in describing the number of the constituent quark scaled elliptic flow $v_2(p_T)/n$ for different hadron species in the small systems created at the LHC.

IV. SUMMARY

In this paper, we study the differential elliptic flow and its NCQ scaling of identified hadrons in 0 – 20% p-Pb collisions at $\sqrt{s_{NN}} = 5.02$ TeV and in $105 < N_{ch} < 150$ p-p collisions at $\sqrt{s_{NN}} = 13$ TeV, us-

ing the **Hydro-Coal-Frag** model that combines hydrodynamics to produce low p_T hadrons, quark coalescence model to produce intermediate p_T hadrons, and LBT string fragmentations to produce high p_T hadrons. The quark coalescence process consists of the recombination of thermal-thermal, thermal-hard, and hard-hard partons, which are generated by the VISH2+1 hydrodynamic model and the LBT model, respectively.

With the combined hadron production procedure, the **Hydro-Coal-Frag** model quantitatively fits the transverse momentum spectrum of identified hadrons below 6 GeV in both p-Pb and p-p collisions. For the collective flow, the **Hydro-Coal-Frag** model nicely describes the differential elliptic flow for identified hadrons from 0-6 GeV and the NCQ scaling of the elliptic flow at intermediate p_T in 0-20% p-Pb collisions. With the quark coalescence, it also shows a grouping behavior of $v_2(p_T)$ between mesons and baryons, where $v_2(p_T)$ of π and K roughly overlap and $v_2(p_T)$ of P and Λ roughly overlap above 2.5 GeV. Meanwhile, we also found that the contribution from string fragmentation and resonance decays slightly breaks the NCQ scaling of v_2 in high multiplicity p-Pb collisions. For p-p collisions, the **Hydro-Coal-Frag** model roughly describes the differential elliptic flow of identified hadrons with properly tuned parameters. However, the quark coalescence contributions at intermediate p_T become smaller, leading to a noticeable violation of the NCQ scaling of v_2 in p-p collisions, as observed in the experiment.

Comparison runs of the **Hydro-Frag** model without the quark coalescence process show that, regardless param-

eter adjustments, the **Hydro-Frag** model cannot simultaneously describe the transverse momentum spectrum and the differential elliptic flow of identified hadrons in either p-Pb or p-p collisions, which underestimates the magnitude of $v_2(p_T)$ at intermediate and high p_T regimes and also violates the NCQ scaling behavior of v_2 for both p-Pb and p-p collisions. It thus demonstrates the importance of quark coalescence in describing the elliptic flow of different hadrons in the intermediate transverse momentum regime. The calculations in this paper also provide support for the existence of the partonic degrees of freedom and the possible formation of the QGP in the high multiplicity p-Pb collisions and p-p collisions at the LHC.

V. ACKNOWLEDGMENTS

This work is supported by the NSFC under grant Nos. 12247107 and 12075007. W.B.Z. is supported by the National Science Foundation (NSF) under grant numbers ACI-2004571 within the framework of the XSCAPE project of the JETSCAPE collaboration and US DOE under Contract No. DE-AC02-05CH11231, and within the framework of the Saturated Glue (SURGE) Topical Theory Collaboration. We also acknowledge the computing resources provided by the SCCAS and Tianhe-1A Super-computing Platform in China and the High-performance Computing Platform of Peking University.

-
- [1] M. Gyulassy, The QGP discovered at RHIC, in *NATO Advanced Study Institute: Structure and Dynamics of Elementary Matter* (2004) pp. 159-182, [arXiv:nucl-th/0403032](#).
 - [2] J. Adams *et al.* (STAR), Experimental and theoretical challenges in the search for the quark gluon plasma: The STAR Collaboration's critical assessment of the evidence from RHIC collisions, *Nucl. Phys. A* **757**, 102 (2005), [arXiv:nucl-ex/0501009](#).
 - [3] B. Muller and J. L. Nagle, Results from the relativistic heavy ion collider, *Ann. Rev. Nucl. Part. Sci.* **56**, 93 (2006), [arXiv:nucl-th/0602029](#).
 - [4] The Frontiers of Nuclear Science, A Long Range Plan, (2008), [arXiv:0809.3137 \[nucl-ex\]](#).
 - [5] P. Jacobs, D. Kharzeev, B. Muller, J. Nagle, K. Rajagopal, and S. Vigdor, Phases of QCD: Summary of the Rutgers long range plan town meeting, January 12-14, 2007, (2007), [arXiv:0705.1930 \[nucl-ex\]](#).
 - [6] U. Heinz and R. Snellings, Collective flow and viscosity in relativistic heavy-ion collisions, *Ann. Rev. Nucl. Part. Sci.* **63**, 123 (2013), [arXiv:1301.2826 \[nucl-th\]](#).
 - [7] C. Gale, S. Jeon, and B. Schenke, Hydrodynamic Modeling of Heavy-Ion Collisions, *Int. J. Mod. Phys. A* **28**, 1340011 (2013), [arXiv:1301.5893 \[nucl-th\]](#).
 - [8] E. Shuryak, Strongly coupled quark-gluon plasma in heavy ion collisions, *Rev. Mod. Phys.* **89**, 035001 (2017), [arXiv:1412.8393 \[hep-ph\]](#).
 - [9] H. Song, Hydrodynamic modelling for relativistic heavy-ion collisions at RHIC and LHC, *Pramana* **84**, 703 (2015), [arXiv:1401.0079 \[nucl-th\]](#).
 - [10] H. Song, Y. Zhou, and K. Gajdosova, Collective flow and hydrodynamics in large and small systems at the LHC, *Nucl. Sci. Tech.* **28**, 99 (2017), [arXiv:1703.00670 \[nucl-th\]](#).
 - [11] V. Khachatryan *et al.* (CMS), Measurement of long-range near-side two-particle angular correlations in pp collisions at $\sqrt{s} = 13$ TeV, *Phys. Rev. Lett.* **116**, 172302 (2016), [arXiv:1510.03068 \[nucl-ex\]](#).
 - [12] G. Aad *et al.* (ATLAS), Observation of Long-Range Elliptic Azimuthal Anisotropies in $\sqrt{s} = 13$ and 2.76 TeV *pp* Collisions with the ATLAS Detector, *Phys. Rev. Lett.* **116**, 172301 (2016), [arXiv:1509.04776 \[hep-ex\]](#).
 - [13] G. Aad *et al.* (ATLAS), Measurement with the ATLAS detector of multi-particle azimuthal correlations in p+Pb collisions at $\sqrt{s_{NN}} = 5.02$ TeV, *Phys. Lett. B* **725**, 60 (2013), [arXiv:1303.2084 \[hep-ex\]](#).
 - [14] V. Khachatryan *et al.* (CMS), Evidence for Collective Multiparticle Correlations in p-Pb Collisions, *Phys. Rev. Lett.* **115**, 012301 (2015), [arXiv:1502.05382 \[nucl-ex\]](#).
 - [15] S. Acharya *et al.* (ALICE), Investigations of Anisotropic Flow Using Multiparticle Azimuthal Correlations in pp, p-Pb, Xe-Xe, and Pb-Pb Collisions at the LHC, *Phys.*

- Rev. Lett. **123**, 142301 (2019), arXiv:1903.01790 [nucl-ex].
- [16] V. Khachatryan *et al.* (CMS), Observation of Long-Range Near-Side Angular Correlations in Proton-Proton Collisions at the LHC, *JHEP* **09**, 091, arXiv:1009.4122 [hep-ex].
- [17] S. Chatrchyan *et al.* (CMS), Observation of Long-Range Near-Side Angular Correlations in Proton-Lead Collisions at the LHC, *Phys. Lett. B* **718**, 795 (2013), arXiv:1210.5482 [nucl-ex].
- [18] B. Abelev *et al.* (ALICE), Long-range angular correlations on the near and away side in p -Pb collisions at $\sqrt{s_{NN}} = 5.02$ TeV, *Phys. Lett. B* **719**, 29 (2013), arXiv:1212.2001 [nucl-ex].
- [19] V. Khachatryan *et al.* (CMS), Evidence for collectivity in pp collisions at the LHC, *Phys. Lett. B* **765**, 193 (2017), arXiv:1606.06198 [nucl-ex].
- [20] B. B. Abelev *et al.* (ALICE), Multiparticle azimuthal correlations in p -Pb and Pb-Pb collisions at the CERN Large Hadron Collider, *Phys. Rev. C* **90**, 054901 (2014), arXiv:1406.2474 [nucl-ex].
- [21] B. B. Abelev *et al.* (ALICE), Long-range angular correlations of π , K and p in p -Pb collisions at $\sqrt{s_{NN}} = 5.02$ TeV, *Phys. Lett. B* **726**, 164 (2013), arXiv:1307.3237 [nucl-ex].
- [22] V. Khachatryan *et al.* (CMS), Long-range two-particle correlations of strange hadrons with charged particles in p Pb and PbPb collisions at LHC energies, *Phys. Lett. B* **742**, 200 (2015), arXiv:1409.3392 [nucl-ex].
- [23] P. Bozek, Collective flow in p -Pb and d -Pd collisions at TeV energies, *Phys. Rev. C* **85**, 014911 (2012), arXiv:1112.0915 [hep-ph].
- [24] J. L. Nagle, A. Adare, S. Beckman, T. Koblesky, J. Orjuela Koop, D. McGlinchey, P. Romatschke, J. Carlson, J. E. Lynn, and M. McCumber, Exploiting Intrinsic Triangular Geometry in Relativistic He3+Au Collisions to Disentangle Medium Properties, *Phys. Rev. Lett.* **113**, 112301 (2014), arXiv:1312.4565 [nucl-th].
- [25] B. Schenke and R. Venugopalan, Eccentric protons? Sensitivity of flow to system size and shape in $p+p$, $p+Pb$ and $Pb+Pb$ collisions, *Phys. Rev. Lett.* **113**, 102301 (2014), arXiv:1405.3605 [nucl-th].
- [26] C. Shen, J.-F. Paquet, G. S. Denicol, S. Jeon, and C. Gale, Collectivity and electromagnetic radiation in small systems, *Phys. Rev. C* **95**, 014906 (2017), arXiv:1609.02590 [nucl-th].
- [27] W. Zhao, Y. Zhou, H. Xu, W. Deng, and H. Song, Hydrodynamic collectivity in proton-proton collisions at 13 TeV, *Phys. Lett. B* **780**, 495 (2018), arXiv:1801.00271 [nucl-th].
- [28] H. Mäntysaari, B. Schenke, C. Shen, and P. Tribedy, Imprints of fluctuating proton shapes on flow in proton-lead collisions at the LHC, *Phys. Lett. B* **772**, 681 (2017), arXiv:1705.03177 [nucl-th].
- [29] K. Werner, B. Guiot, I. Karpenko, and T. Pierog, Analysing radial flow features in p -Pb and p - p collisions at several TeV by studying identified particle production in EPOS3, *Phys. Rev. C* **89**, 064903 (2014), arXiv:1312.1233 [nucl-th].
- [30] G.-Y. Qin and B. Müller, Elliptic and triangular flow anisotropy in deuteron-gold collisions at $\sqrt{s_{NN}} = 200$ GeV at RHIC and in proton-lead collisions at $\sqrt{s_{NN}} = 5.02$ TeV at the LHC, *Phys. Rev. C* **89**, 044902 (2014), arXiv:1306.3439 [nucl-th].
- [31] Y. Zhou, X. Zhu, P. Li, and H. Song, Investigation of possible hadronic flow in $\sqrt{s_{NN}} = 5.02$ TeV $p-Pb$ collisions, *Phys. Rev. C* **91**, 064908 (2015), arXiv:1503.06986 [nucl-th].
- [32] P. Bozek, A. Bzdak, and G.-L. Ma, Rapidity dependence of elliptic and triangular flow in proton-nucleus collisions from collective dynamics, *Phys. Lett. B* **748**, 301 (2015), arXiv:1503.03655 [hep-ph].
- [33] R. D. Weller and P. Romatschke, One fluid to rule them all: viscous hydrodynamic description of event-by-event central $p+p$, $p+Pb$ and $Pb+Pb$ collisions at $\sqrt{s} = 5.02$ TeV, *Phys. Lett. B* **774**, 351 (2017), arXiv:1701.07145 [nucl-th].
- [34] W. Zhao, Y. Zhou, K. Murase, and H. Song, Searching for small droplets of hydrodynamic fluid in proton-proton collisions at the LHC, *Eur. Phys. J. C* **80**, 846 (2020), arXiv:2001.06742 [nucl-th].
- [35] A. Bzdak and G.-L. Ma, Elliptic and triangular flow in $p+Pb$ and peripheral $Pb+Pb$ collisions from parton scatterings, *Phys. Rev. Lett.* **113**, 252301 (2014), arXiv:1406.2804 [hep-ph].
- [36] A. Kurkela, U. A. Wiedemann, and B. Wu, Nearly isentropic flow at sizeable η/s , *Phys. Lett. B* **783**, 274 (2018), arXiv:1803.02072 [hep-ph].
- [37] W. Zhao, S. Ryu, C. Shen, and B. Schenke, 3D structure of anisotropic flow in small collision systems at energies available at the BNL Relativistic Heavy Ion Collider, *Phys. Rev. C* **107**, 014904 (2023), arXiv:2211.16376 [nucl-th].
- [38] W. Zhao, C. Shen, and B. Schenke, Collectivity in Ultraperipheral $Pb+Pb$ Collisions at the Large Hadron Collider, *Phys. Rev. Lett.* **129**, 252302 (2022), arXiv:2203.06094 [nucl-th].
- [39] Z. Wu, B. Fu, S. Zhao, R. Liu, and H. Song, Collective flow and the fluid behavior in $p/d/{}^3\text{He}+Au$ collisions at $\sqrt{s_{NN}} = 200$ GeV, (2023), arXiv:2307.02995 [nucl-th].
- [40] K. Dusling and R. Venugopalan, Azimuthal collimation of long range rapidity correlations by strong color fields in high multiplicity hadron-hadron collisions, *Phys. Rev. Lett.* **108**, 262001 (2012), arXiv:1201.2658 [hep-ph].
- [41] K. Muneyuki and N. Ohta, Unitarity versus Renormalizability of Higher Derivative Gravity in 3D, *Phys. Rev. D* **85**, 101501 (2012), arXiv:1201.2058 [hep-th].
- [42] K. Dusling and R. Venugopalan, Evidence for BFKL and saturation dynamics from dihadron spectra at the LHC, *Phys. Rev. D* **87**, 051502 (2013), arXiv:1210.3890 [hep-ph].
- [43] A. Kovner and M. Lublinsky, Angular and long range rapidity correlations in particle production at high energy, *Int. J. Mod. Phys. E* **22**, 1330001 (2013), arXiv:1211.1928 [hep-ph].
- [44] Y. V. Kovchegov and D. E. Wertepny, Long-Range Rapidity Correlations in Heavy-Light Ion Collisions, *Nucl. Phys. A* **906**, 50 (2013), arXiv:1212.1195 [hep-ph].
- [45] B. Schenke, S. Schlichting, and R. Venugopalan, Azimuthal anisotropies in $p+Pb$ collisions from classical Yang-Mills dynamics, *Phys. Lett. B* **747**, 76 (2015), arXiv:1502.01331 [hep-ph].
- [46] T. Lappi, B. Schenke, S. Schlichting, and R. Venugopalan, Tracing the origin of azimuthal gluon correlations in the color glass condensate, *JHEP* **01**, 061, arXiv:1509.03499 [hep-ph].
- [47] B. Schenke, S. Schlichting, P. Tribedy, and R. Venugopalan, Mass ordering of spectra from fragmentation

- of saturated gluon states in high multiplicity proton-proton collisions, *Phys. Rev. Lett.* **117**, 162301 (2016), [arXiv:1607.02496 \[hep-ph\]](#).
- [48] K. Dusling, M. Mace, and R. Venugopalan, Multiparticle collectivity from initial state correlations in high energy proton-nucleus collisions, *Phys. Rev. Lett.* **120**, 042002 (2018), [arXiv:1705.00745 \[hep-ph\]](#).
- [49] K. Dusling, M. Mace, and R. Venugopalan, Parton model description of multiparticle azimuthal correlations in pA collisions, *Phys. Rev. D* **97**, 016014 (2018), [arXiv:1706.06260 \[hep-ph\]](#).
- [50] M. Mace, V. V. Skokov, P. Tribedy, and R. Venugopalan, Systematics of azimuthal anisotropy harmonics in proton-nucleus collisions at the LHC from the Color Glass Condensate, *Phys. Lett. B* **788**, 161 (2019), [Erratum: *Phys.Lett.B* 799, 135006 (2019)], [arXiv:1807.00825 \[hep-ph\]](#).
- [51] B. Schenke, The smallest fluid on Earth, *Rept. Prog. Phys.* **84**, 082301 (2021), [arXiv:2102.11189 \[nucl-th\]](#).
- [52] J. L. Albacete *et al.*, Predictions for $p+Pb$ Collisions at $\sqrt{s_{NN}} = 5$ TeV: Comparison with Data, *Int. J. Mod. Phys. E* **25**, 1630005 (2016), [arXiv:1605.09479 \[hep-ph\]](#).
- [53] K. J. Eskola, P. Paakkinen, H. Paukkunen, and C. A. Salgado, EPPS16: Nuclear parton distributions with LHC data, *Eur. Phys. J. C* **77**, 163 (2017), [arXiv:1612.05741 \[hep-ph\]](#).
- [54] V. Pacik (ALICE), Elliptic flow of identified hadrons in small collisional systems measured with ALICE, *Nucl. Phys. A* **982**, 451 (2019), [arXiv:1807.04538 \[nucl-ex\]](#).
- [55] A. M. Sirunyan *et al.* (CMS), Elliptic flow of charm and strange hadrons in high-multiplicity pPb collisions at $\sqrt{s_{NN}} = 8.16$ TeV, *Phys. Rev. Lett.* **121**, 082301 (2018), [arXiv:1804.09767 \[hep-ex\]](#).
- [56] W. Zhao, C. M. Ko, Y.-X. Liu, G.-Y. Qin, and H. Song, Probing the Partonic Degrees of Freedom in High-Multiplicity $p-Pb$ collisions at $\sqrt{s_{NN}} = 5.02$ TeV, *Phys. Rev. Lett.* **125**, 072301 (2020), [arXiv:1911.00826 \[nucl-th\]](#).
- [57] W. Zhao, C. M. Ko, Y.-X. Liu, G.-Y. Qin, and H. Song, Number of constituent quark scaling of elliptic flows in high multiplicity $p-Pb$ collisions at $\sqrt{s_{NN}} = 5.02$ TeV, *Nucl. Phys. A* **1005**, 121876 (2021), [arXiv:2001.10689 \[nucl-th\]](#).
- [58] W. Zhao, W. Ke, W. Chen, T. Luo, and X.-N. Wang, From Hydrodynamics to Jet Quenching, Coalescence, and Hadron Cascade: A Coupled Approach to Solving the RAA \otimes v2 Puzzle, *Phys. Rev. Lett.* **128**, 022302 (2022), [arXiv:2103.14657 \[hep-ph\]](#).
- [59] S. Acharya *et al.* (ALICE), Multiplicity dependence of π , K, and p production in pp collisions at $\sqrt{s} = 13$ TeV, *Eur. Phys. J. C* **80**, 693 (2020), [arXiv:2003.02394 \[nucl-ex\]](#).
- [60] M. Aaboud *et al.* (ATLAS), Measurements of long-range azimuthal anisotropies and associated Fourier coefficients for pp collisions at $\sqrt{s} = 5.02$ and 13 TeV and $p+Pb$ collisions at $\sqrt{s_{NN}} = 5.02$ TeV with the ATLAS detector, *Phys. Rev. C* **96**, 024908 (2017), [arXiv:1609.06213 \[nucl-ex\]](#).
- [61] J. S. Moreland, J. E. Bernhard, and S. A. Bass, Alternative ansatz to wounded nucleon and binary collision scaling in high-energy nuclear collisions, *Phys. Rev. C* **92**, 011901 (2015), [arXiv:1412.4708 \[nucl-th\]](#).
- [62] U. W. Heinz, H. Song, and A. K. Chaudhuri, Dissipative hydrodynamics for viscous relativistic fluids, *Phys. Rev. C* **73**, 034904 (2006), [arXiv:nucl-th/0510014](#).
- [63] H. Song and U. W. Heinz, Suppression of elliptic flow in a minimally viscous quark-gluon plasma, *Phys. Lett. B* **658**, 279 (2008), [arXiv:0709.0742 \[nucl-th\]](#).
- [64] H. Song and U. W. Heinz, Causal viscous hydrodynamics in 2+1 dimensions for relativistic heavy-ion collisions, *Phys. Rev. C* **77**, 064901 (2008), [arXiv:0712.3715 \[nucl-th\]](#).
- [65] H. Song, *Causal Viscous Hydrodynamics for Relativistic Heavy Ion Collisions*, Other thesis (2009), [arXiv:0908.3656 \[nucl-th\]](#).
- [66] C. Shen, Z. Qiu, H. Song, J. Bernhard, S. Bass, and U. Heinz, The iEBE-VISHNU code package for relativistic heavy-ion collisions, *Comput. Phys. Commun.* **199**, 61 (2016), [arXiv:1409.8164 \[nucl-th\]](#).
- [67] T. Sjostrand, S. Mrenna, and P. Z. Skands, A Brief Introduction to PYTHIA 8.1, *Comput. Phys. Commun.* **178**, 852 (2008), [arXiv:0710.3820 \[hep-ph\]](#).
- [68] X.-N. Wang and Y. Zhu, Medium Modification of γ -jets in High-energy Heavy-ion Collisions, *Phys. Rev. Lett.* **111**, 062301 (2013), [arXiv:1302.5874 \[hep-ph\]](#).
- [69] J. J. Peng, Y. Lu, B. H. Sun, and Y. M. Zhao, New charge radius relations for atomic nuclei, *Phys. Rev. C* **90**, 054318 (2014), [Erratum: *Phys.Rev.C* 91, 019902 (2015)], [arXiv:1408.6954 \[nucl-th\]](#).
- [70] S. Cao, T. Luo, G.-Y. Qin, and X.-N. Wang, Linearized Boltzmann transport model for jet propagation in the quark-gluon plasma: Heavy quark evolution, *Phys. Rev. C* **94**, 014909 (2016), [arXiv:1605.06447 \[nucl-th\]](#).
- [71] W.-J. Xing, S. Cao, G.-Y. Qin, and H. Xing, Flavor hierarchy of jet quenching in relativistic heavy-ion collisions, *Phys. Lett. B* **805**, 135424 (2020), [arXiv:1906.00413 \[hep-ph\]](#).
- [72] S. A. Bass *et al.*, Microscopic models for ultrarelativistic heavy ion collisions, *Prog. Part. Nucl. Phys.* **41**, 255 (1998), [arXiv:nucl-th/9803035](#).
- [73] H. Song and U. W. Heinz, Multiplicity scaling in ideal and viscous hydrodynamics, *Phys. Rev. C* **78**, 024902 (2008), [arXiv:0805.1756 \[nucl-th\]](#).
- [74] P. Huovinen and P. Petreczky, QCD Equation of State and Hadron Resonance Gas, *Nucl. Phys. A* **837**, 26 (2010), [arXiv:0912.2541 \[hep-ph\]](#).
- [75] C. Shen, U. Heinz, P. Huovinen, and H. Song, Systematic parameter study of hadron spectra and elliptic flow from viscous hydrodynamic simulations of Au+Au collisions at $\sqrt{s_{NN}} = 200$ GeV, *Phys. Rev. C* **82**, 054904 (2010), [arXiv:1010.1856 \[nucl-th\]](#).
- [76] J. E. Bernhard, J. S. Moreland, S. A. Bass, J. Liu, and U. Heinz, Applying Bayesian parameter estimation to relativistic heavy-ion collisions: simultaneous characterization of the initial state and quark-gluon plasma medium, *Phys. Rev. C* **94**, 024907 (2016), [arXiv:1605.03954 \[nucl-th\]](#).
- [77] J. S. Moreland, J. E. Bernhard, and S. A. Bass, Bayesian calibration of a hybrid nuclear collision model using p-Pb and Pb-Pb data at energies available at the CERN Large Hadron Collider, *Phys. Rev. C* **101**, 024911 (2020), [arXiv:1808.02106 \[nucl-th\]](#).
- [78] H. Song, S. A. Bass, and U. Heinz, Viscous QCD matter in a hybrid hydrodynamic+Boltzmann approach, *Phys. Rev. C* **83**, 024912 (2011), [arXiv:1012.0555 \[nucl-th\]](#).
- [79] X. Li, W.-J. Fu, and Y.-X. Liu, Thermodynamics of 2+1 Flavor Polyakov-Loop Quark-Meson Model under External Magnetic Field, *Phys. Rev. D* **99**, 074029 (2019),

- arXiv:1902.03866 [hep-ph].
- [80] J. D. Carroll, D. B. Leinweber, A. G. Williams, and A. W. Thomas, Phase Transition from QMC Hyperonic Matter to Deconfined Quark Matter, *Phys. Rev. C* **79**, 045810 (2009), arXiv:0809.0168 [nucl-th].
- [81] F. Gao and Y.-x. Liu, Temperature Effect on Shear and Bulk Viscosities of QCD Matter, *Phys. Rev. D* **97**, 056011 (2018), arXiv:1702.01420 [hep-ph].
- [82] W.-j. Fu, J. M. Pawłowski, and F. Rennecke, QCD phase structure at finite temperature and density, *Phys. Rev. D* **101**, 054032 (2020), arXiv:1909.02991 [hep-ph].
- [83] P. Levai and U. W. Heinz, Massive gluons and quarks and the equation of state obtained from SU(3) lattice QCD, *Phys. Rev. C* **57**, 1879 (1998), arXiv:hep-ph/9710463.
- [84] M. Zhao, **Pinning down the origin of collectivity in small systems with ALICE**, presented at Quark Matter 2023.
- [85] W. Chen, S. Cao, T. Luo, L.-G. Pang, and X.-N. Wang, Effects of jet-induced medium excitation in γ -hadron correlation in A+A collisions, *Phys. Lett. B* **777**, 86 (2018), arXiv:1704.03648 [nucl-th].
- [86] T. Luo, S. Cao, Y. He, and X.-N. Wang, Multiple jets and γ -jet correlation in high-energy heavy-ion collisions, *Phys. Lett. B* **782**, 707 (2018), arXiv:1803.06785 [hep-ph].
- [87] Y. He, T. Luo, X.-N. Wang, and Y. Zhu, Linear Boltzmann Transport for Jet Propagation in the Quark-Gluon Plasma: Elastic Processes and Medium Recoil, *Phys. Rev. C* **91**, 054908 (2015), [Erratum: *Phys. Rev. C* **97**, 019902 (2018)], arXiv:1503.03313 [nucl-th].
- [88] S. Cao, T. Luo, G.-Y. Qin, and X.-N. Wang, Heavy and light flavor jet quenching at RHIC and LHC energies, *Phys. Lett. B* **777**, 255 (2018), arXiv:1703.00822 [nucl-th].
- [89] K. C. Han, R. J. Fries, and C. M. Ko, Jet Fragmentation via Recombination of Parton Showers, *Phys. Rev. C* **93**, 045207 (2016), arXiv:1601.00708 [nucl-th].
- [90] J. Beringer *et al.* (Particle Data Group), Review of Particle Physics (RPP), *Phys. Rev. D* **86**, 010001 (2012).
- [91] J. Adam *et al.* (ALICE), Multiplicity dependence of charged pion, kaon, and (anti)proton production at large transverse momentum in p-Pb collisions at $\sqrt{s_{NN}} = 5.02$ TeV, *Phys. Lett. B* **760**, 720 (2016), arXiv:1601.03658 [nucl-ex].